Advances in Materials, Manufacturing, and Repair for Power Plants:
Proceedings from the Tenth International Conference
October 15–18, 2024, Bonita Springs Florida, USA
https://doi.org/10.31399/asm.cp.epri2024p0760

CREEP STRENGTH AND MICROSTRUCTURE IN WELDED JOINTS OF ASME GR.91 TYPE 1 AND TYPE 2 STEELS

Masatoshi Mitsuhara
Kyushu University, Fukuoka, Japan

Katsuhiro Sato
IHI Corporation, Kanagawa, Japan

Kyohei Nomura
IHI Corporation, Kanagawa, Japan

Takahiro Kimura
IHI Corporation, Kanagawa, Japan

Yoshiki Shioda
IHI Corporation, Kanagawa, Japan

Kota Sawada
National Institute for Materials Science, Tsukuba, Japan

Kazuhiro Kimura
National Institute for Materials Science, Tsukuba, Japan

Hideharu Nakashima
Kyushu University, Fukuoka, Japan

ABSTRACT

Creep strength of welded joints of Grade 91 Type 1 and Type 2 steels was evaluated; impurity elements in the Type 1 steel reduced the creep strength. This reduction was attributed to an increase in the amount of residual carbides in the fine-grain heat-affected zone during welding.

INTRODUCTION

The creep strength enhanced ferritic (CSEF) heat-resistant steels containing high-chromium (Cr), such as ASME Gr.91 steel, are used for steam pipes in thermal power plants. ASME (2019) divided Gr.91 steel into two standards: conventional Type 1 and newly-established Type 2[1]. Type 2 steel is a heat-resistant steel with reduced impurity elements to improve creep ductility. In this study, creep strength and microstructure in welded joints of conventional Gr. 91 Type 1 steel and the new standard Type 2 steel were compared. During welding, the heat input from the weld metal produces a heat-affected zone (HAZ) in which the microstructure of the base metal changes continuously. The HAZ microstructure distribution can be distinguished from the weld metal (WM) side as follows: coarse-grained HAZ (CGHAZ), fine-grained HAZ (FGHAZ), intercritical HAZ (ICHAZ), which is partial transformation zone, and base metal (BM). Although CSEF steels have excellent high-temperature strength, they typically experience a significant reduction in this strength in the HAZ that is formed from welding[2]. In addition, much remains unknown about the effect of impurity elements on the creep strength of welded joints. Therefore, in this study, the creep strength of welded joints of Type 1 and Type 2 steels were compared and the differences in their strength were discussed in terms of microstructural changes.

EXPETIMENTAL PROCEDURE

Two steels were prepared for creep test: one was the impurity element free steel satisfying Type 2 and the other was impurity element added steel doing Type 1. Their chemical compositions are shown in Table 1. After welded joints of these steels were fabricated, post weld heat treatment (PWHT) was performed at 760°C for 4 h to reduce residual stress. Cross weld creep test specimens were cut from the welded joint with the HAZ positioned in the center of the parallel portion, and creep rupture tests were carried out at a temperature of 650°C and stresses of 40-80 MPa. In addition, a creep interruption test was also performed to investigate microstructural changes during deformation. Mechanical and chemical polishing was performed on the specimens before and after the creep test to ensure a clean, strain-free specimen surface. Scanning electron microscopy (SEM) was used to observe the microstructure, and electron back-scatter diffraction (EBSD) method was used to obtain the crystal orientation information. Vickers hardness test was also conducted to measure the hardness change of HAZ.

Table 1: Chemical compositions of specimens (mass%).

	C	Si	Mn	P	S	Ni	Cr	Mo	V	Nb	Sol-Al	N	Sb	As	Sn
Type 2 steel	0.087	0.29	0.41	0.011	0.0005	0.09	8.49	0.93	0.20	0.074	0.007	0.052	<0.001	<0.001	<0.001
Type 1 steel	0.082	0.30	0.41	0.012	0.0006	0.11	8.45	0.94	0.20	0.080	0.008	0.052	0.008	0.019	0.018

RESULTS AND DISCUSSION

Figure 1 shows the creep rupture test results for Type 1 and Type 2 steels. Under all creep test conditions conducted in this study, Type 2 steel exhibits superior creep strength (longer rupture time) than Type 1 steel. In other words, impurity elements are clearly shown to contribute to the reduction of creep strength of welded joints.

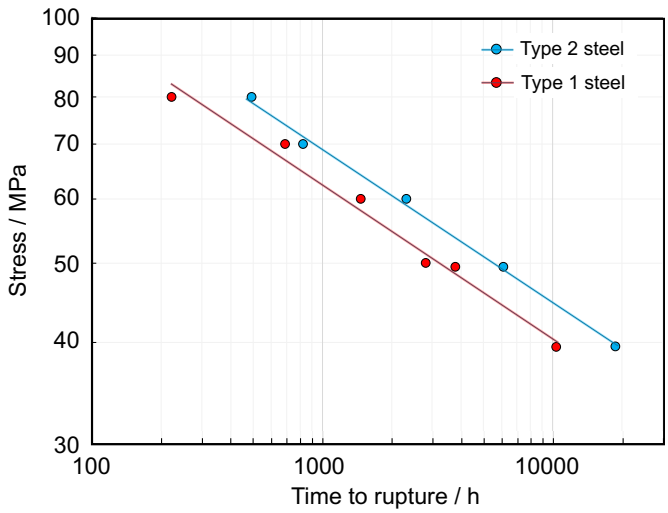

Figure 1: Relationships between stress and rupture time in creep tests at 650˚C.

Observation of creep ruptures showed that the rupture location for both steels was at the FGHAZ under the present experimental conditions. Figure 2 shows the crystal orientation distribution maps at the FGHAZ for the initial (after PWHT) and creep-interrupted (650˚C-50 MPa, interrupted time: 1000 h, 2000 h, and 3000 h) Type 2 steel. The Vickers hardness is appended in the upper left corner of each map. Figure 3 shows the frequency distribution of misorientation in the same field of view as that shown in Fig. 2. Before welding, this steel has a lath martensitic structure, which is known to have a peak at 50-60° in the misorientation frequency distribution[3]. A similar peak is observed in the FGHAZ of the initial (after PWHT) and 1000 h creep-interrupted specimens, indicating that the lath martensitic structure is maintained in the FGHAZ after PWHT. On the other hand, in the 2000 h and 3000 h creep-interrupted specimens, peaks specific to lath martensitic microstructure are hardly observed, and the hardness also decreases gradually with creep time. This indicates that the ferrite formation caused by dynamic recrystallization and its grain growth occurred during creep. It is inferred that the formation of ferrite grains in the FGHAZ contributed to the decrease in creep strength.

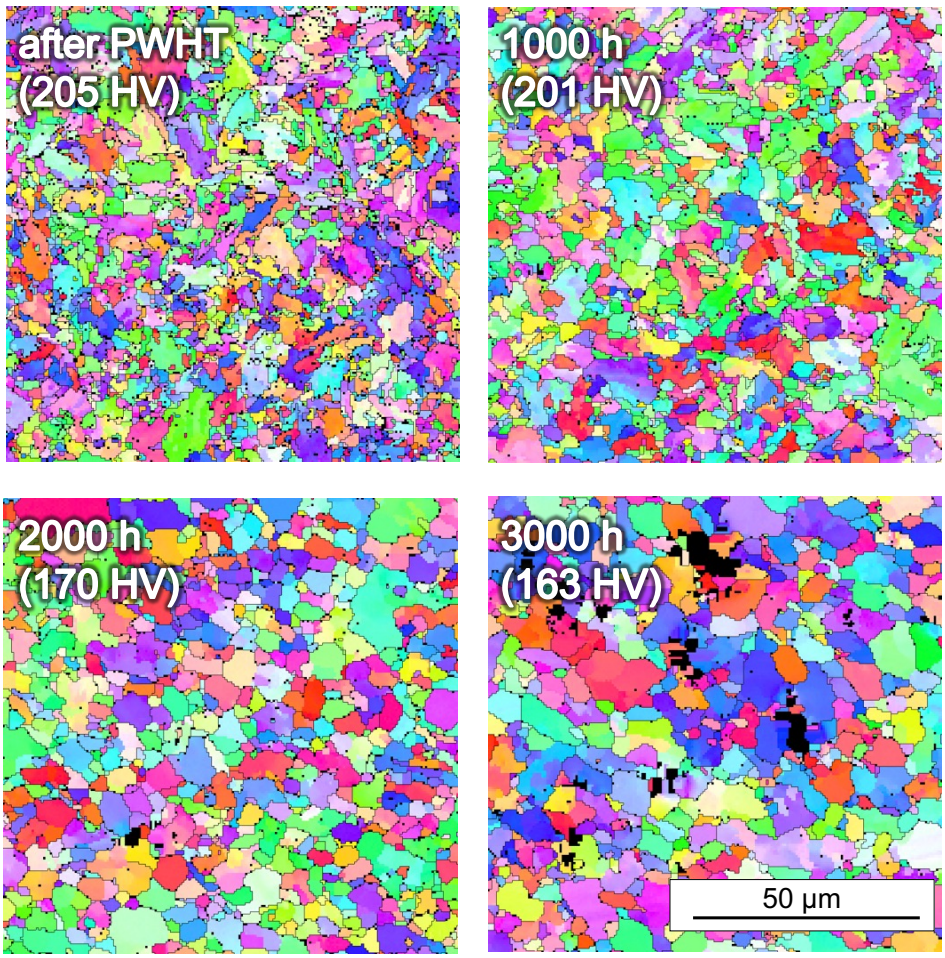

Figure 2: Crystal orientation distribution maps in the FGHAZ of Type 2 steel before and after creep test.

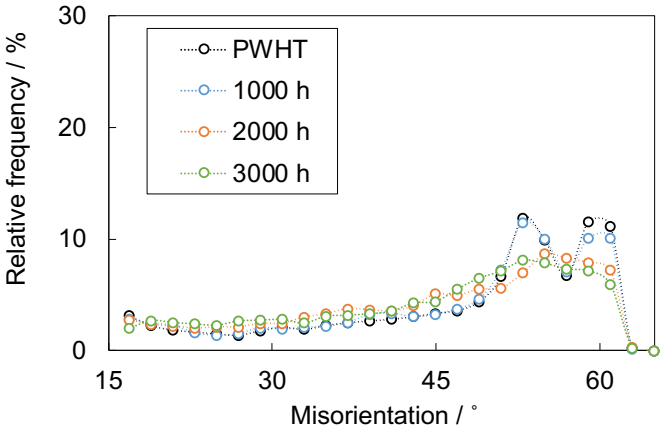

Figure 3: Changes of relative frequency of misorientation during creep test.

Since carbides (mainly $M_{23}C_6$ carbides) on grain boundaries are strongly involved in the behavior of ferrite formation and grain growth, the dispersion of $M_{23}C_6$ carbides near the FGHAZ of Type 1 and Type 2 steels after welding and PWHT is shown in Fig. 4. In the same figure, the volume fraction of $M_{23}C_6$ carbides in Type 2 steel calculated by thermal equilibrium state calculation is also shown. In the as-welded data, solid solution of $M_{23}C_6$ carbides begins in the ICHAZ region heated to temperatures above the A_{C1} point, indicating a slight decrease in carbide volume. As the temperature heated during welding increases (toward the left side of the graph), the solid solution of $M_{23}C_6$ carbides progresses and their amount gradually decreases. On the other hand, after PWHT, the carbide returns to the same amount as indicated by the thermal equilibrium state calculation in all regions. What is important here is the difference between the amount of carbides in the as-welded condition and that after PWHT. This is because the amount of carbides indicated by the difference has a strong influence on the suppression of ferrite formation and its growth during creep deformation, and thus on the creep strength of the weld joint.

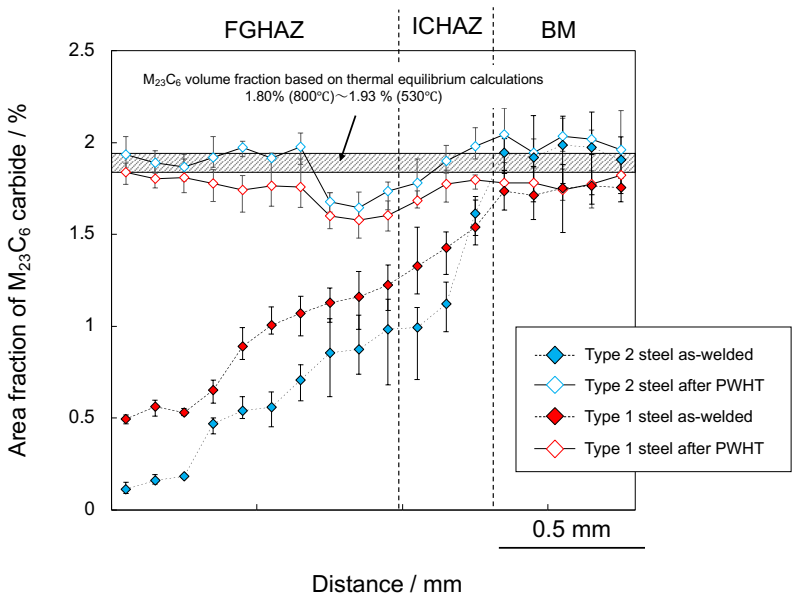

Figure 4: Changes of area fraction of $M_{23}C_6$ carbides during welding process.

Figure 5 shows the microstructures of the FGHAZ of Type 2 steel as-welded and after PWHT, where the prior γ grains are smaller because the FGHAZ was once heated to just above the A_{C3} point by the welding heat and then transformed to martensite again. Interestingly, $M_{23}C_6$ carbides are observed in rows ignoring the prior γ grains. These are $M_{23}C_6$ carbides that precipitated on the prior γ grain boundary before welding. The amount of $M_{23}C_6$ carbides precipitating on the grain boundary of the current lath martensitic structure in PWHT is clearly reduced due to the residual $M_{23}C_6$ carbides. The tendencies of the $M_{23}C_6$ carbide dispersion state and microstructural changes during creep deformation were similar for Type 1 and Type 2 steels. However, as shown in Fig. 1, the addition of impurities clearly reduced the creep strength, and as shown in Fig. 4, the amount of $M_{23}C_6$ carbides remaining after welding increased in the FGHAZ of Type 1 steel compared to that of Type 2 steel. Therefore, the amount of $M_{23}C_6$ carbides precipitating on the grain boundary after PWHT is smaller. This implies that the amount of carbides contributing to microstructural stabilization during creep deformation is relatively low, and as a result, it can be concluded that in Type 1 steels, early recovery and recrystallization of the microstructure during creep deformation caused the reduction in creep strength. The intergranular diffusion rate of the metal elements constituting the carbides plays a role in the residual carbides during welding; some of the impurity elements abundant in the Type 1 steel segregate to the grain boundaries and stabilize the grain boundary structure, thereby reducing the intergranular diffusion rate. This is assumed to be involved in the increase of residual carbides in the Type 1 steel.

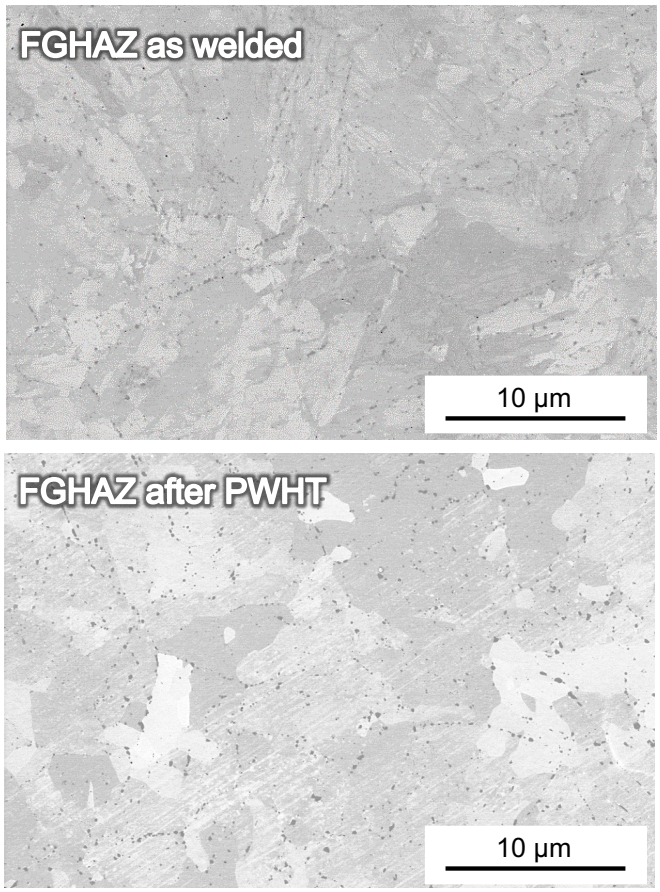

Figure 5: SEM images in the FGHAZ of Type 2 steel as-welded and after PWHT.

CONCLUSIONS

Creep tests and microstructural observations were conducted on Grade 91 Type 1 and Type 2 steels to determine the effects of impurity elements on creep strength. The results obtained are as follows.

1. The creep strength of Type 2 steel was higher than that of Type 1 steel. Therefore, impurity elements were found to reduce creep strength.
2. Under the creep conditions of this study, creep rupture occurred at the FGHAZ, where a microstructural change from martensite to ferrite occurred during creep deformation, as well as growth of its ferrite grains.
3. More carbides remained in the Type 1 steel than in the Type 2 steel in the as-welded condition. Therefore, the amount of carbides precipitating on the grain boundary after PWHT was smaller. This means that the amount of carbides effectively contributing to creep strength was small, which was inferred to be the reason for the lower creep strength of the Type 1 steel.

ACKNOWLEDGMENTS

This work was partially supported by JSPS KAKENHI [grant numbers JP20H02466, JP22H01759].

REFERENCES

[1] ASME Boiler and Pressure Vessel Code, Section II-A, SA387/SA387M Grade 91, 2019.
[2] Yaguchi, M., Nakamura, K., Nakahashi, S., “Re-evaluation of long-term creep strength of welded joint of ASME Grade 91 type steel”, *Proceedings of the ASME 2016 Pressure Vessels and Piping Conference, PVP2016,* Vancouver, British Columbia, Canada, July 2016, PVP2016-63316.
[3] Morito, S., Tanaka, H., Konishi, R., Furuhara, T., Maki, T., “The morphology and crystallography of lath martensite in Fe-C alloys”, Acta Materialia, Vol. 51 (2003), pp. 1789-1799.